 MCB, vol.1, no.2, pp.161-167, 2004

Modeling of Surface-Tension-Driven Flow of Blood in Capillary Tubes

Jun Wang[1], Wei Huang[2], Raghbir S. Bhullar[3], and Pin Tong[2]

Abstract: Surface-tension-driven blood flow into a capillary tube, as in some medical devices, is studied. In a previous article, we considered the early stages of the entry flow from a drop of blood into a capillary, and solved the problem analytically under the assumption that the resistance of the air is negligible. In the present note we consider a capillary tube of finite length, with the far end containing a small window which opens to the atmosphere. The dynamic reverberation of the air in the capillary tube is analyzed in conjunction with the dynamics of the blood. Existing computing programs are used to solve the Navier-Stokes equations. The interface is characterized by the surface tension between the blood and the air, and the contact angle at the triple point where the air-blood interface meets the capillary tube wall. The results tell us how good our earlier simplified analysis is. The new numerical results show that the smaller the window, the larger is the effect of aerodynamic reverberation. However, even for a window as small as 4% of the capillary cross section, and located at the end of the capillary, the difference of the time of arrival of the interface at the window is less than 5%.

keyword: surface-tension-driven blood flow, capillary tube, finite element model

1 Introduction

Surface tension is an important factor in biomechanics when smaller entities are concerned, such as in the capillary blood vessels, cells, interstitial spaces, intracellular structures, and some medical devices. In Fung (1975, 1990, 1993, 1997), some significant cases in physiology are discussed. A case of importance to spacecraft and astronautics is analyzed in Tong and Fung (1965). Fundamental equations are given in Yih (1988). Data on the surface tension of blood in the lung are given in Zupkas (1977), and Thurston (1976). The entry flow is analyzed in Lew and Fung (1969). Some classical results are presented in Purday (1949). In Huang, Bhullar, and Fung (2001), we investigated the surface-tension-driven flow of blood from a droplet into a long air-filled circular or rectangular cylinder, which is a situation that occurs in several commercially available devices for blood glucose measurement. The blood flow in the entry region is analyzed analytically in Huang, Bhullar, and Fung (2001). Our focus was on the events immediately following the touching of a capillary tube with a drop of blood. The surface tension begins to pull the blood into the tube. The inflow accelerates following the contact, and gradually reaches a steady state. To simplify the analysis, we assumed an infinitely long capillary tube, and ignored the dynamics of the airflow ahead of the air-blood interface in Huang, Bhullar, and Fung (2001). The effects of these simplifying assumptions must be evaluated. This evaluation is the purpose of the present paper. Here, we consider a capillary tube of finite length. One end of which is open and is used to touch a drop of blood, the other end is closed but contains a small window that opens to the atmosphere. The configuration is shown in Fig. 1, which is quite close to a realistic medical device. We analyze the flow of blood and air by solving the Navier-Stokes equations with numerical methods, after the process of initial entry of blood into the capillary tube is completed. In other words, the present paper complements that of Huang, Bhullar, and Fung (2001) by a thorough analysis of the motion of air and blood in the capillary according to Navier-Stokes equation.

2 The Problem and Governing Equations

A drop of blood is sucked into and flows in a capillary tube by the surface tension of the blood-air interface as shown in Fig. 1(A). The entry section is a rectangle of finite aspect ratio. After flowing into the capillary of length L, the fluid exits the capillary from a small window, with

[1] Department of Material Science, Fudan University, Shanghai, China
[2] Department of Bioengineering, University of California San Diego, La Jolla, CA 92093-0412
[3] Roche Diagnostics Corporation, Indianapolis, IN 46206

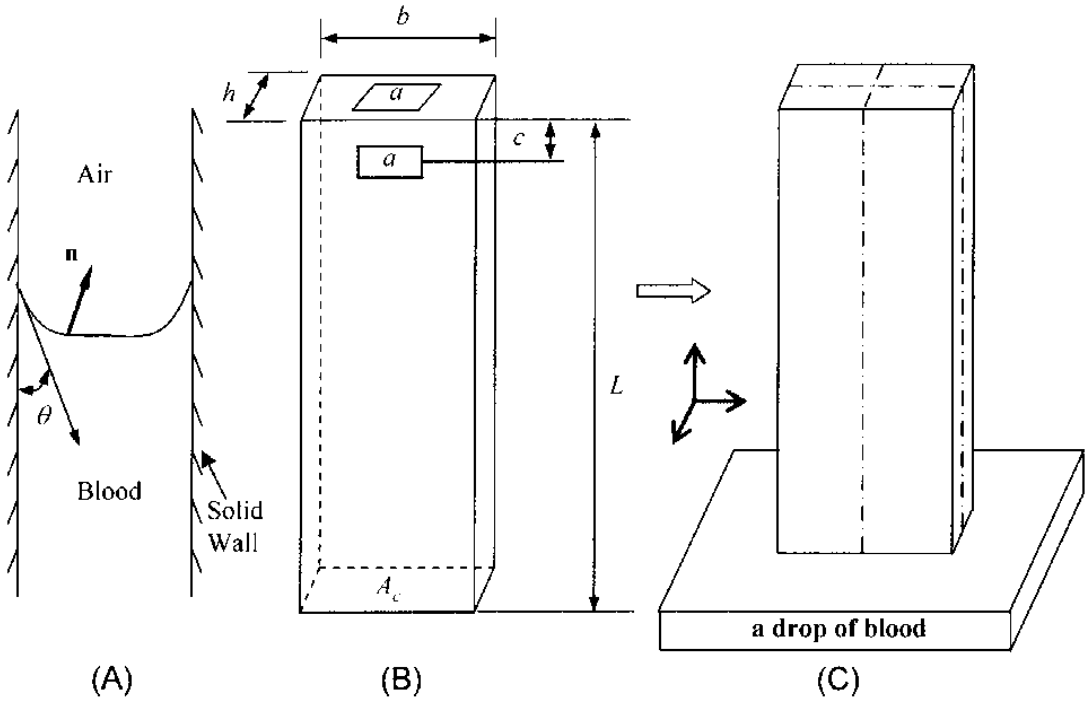

Figure 1 : (A) Interface between two fluids (blood and air) with a contact angle θ in a cylindrical capillary tube. *n* is the normal vector to the interface. A blood droplet was sucked into the tube from the entrance at the bottom and moved to the exit on the top, and the flow of blood in the tube is driven by surface tension. (B) A rectangular capillary tube with a small exit opening, *a*, at the end of the tube or on the side wall. (C) Our computational model involves two-phase fluids: the capillary tube filled with air is dipped into a drop of blood. In the computation model, the capillary tube is divided into 4 equal quarters.

area *a*, either at the top end of the capillary tube, or on a side wall of the tube close to the top end of the tube as shown in Fig. 1(B). The lumen thickness, length, and width of the capillary tube are denoted by *h*, *L*, and *b*, respectively. *c* is the distance from the center of the window on the side wall to the top end of the tube. The flow of the blood and the air in the capillary tube is laminar, and the fluids are considered to be incompressible and homogeneous. The velocity field is represented by (*u*, *v*, *w*) in the (*x*, *y*, *z*) directions, respectively. The initial stages of the flow into a capillary tube from a droplet are analyzed in Huang, Bhullar, and Fung (2001). On the contact of the capillary with a drop of blood, a plane interface is formed, which immediately became curved because of the contact angle and surface tension. Huang, Bhullar, and Fung (2001) analyzed the initial accelerating phase. Soon the acceleration is slowed down, a curved interface is developed, and then the present analysis takes over.

In the present analysis, the blood is assumed to be Newtonian. The blood and air satisfy the Navier-Stokes equations and no-slip boundary conditions. Equations for these are well known [see, e.g., Fung (1993, 1997), Yih (1988), and Purday (1949)] that

$$\rho_\alpha \frac{d\mathbf{u}}{dt} = \rho_\alpha \mathbf{g} - \nabla p_\alpha + \mu_\alpha \nabla^2 \mathbf{u} \ \text{(Momentum Eq.)} \qquad (1)$$

$$\nabla \cdot \mathbf{u} = 0 \ \text{(Continuity Eq.)} \qquad (2)$$

where *t* denotes time, $\frac{d}{dt}$ is the total time derivative, $\mathbf{u}$ is the velocity vector, ∇ is the gradient operator defined as $\nabla = [\partial/\partial x, \partial/\partial y, \partial/\partial z]$, ρ_α is the density, $\mathbf{g}$ is the body force per unit mass, p_α is the pressure and μ_α is the viscosity in the fluid α, where α denotes the air or the liquid In the present study, we assume that the fluids are incompressible and viscous.

We first consider the surface tension effect on the liquid-air interface as shown in Fig. 1(A) with a contact angle θ at the wall. The surface tension induced normal force is

acting on the free surface

$$\mathbf{f} = -\Gamma\kappa\mathbf{n}, \quad \kappa = -\nabla\cdot\mathbf{n}, \tag{3}$$

where $\mathbf{n}$ the unit vector normal to the interface pointed toward the air, Γ is the surface tension coefficient, and κ is the surface curvature. The dynamic conditions, which describe the balance of the normal traction σ_n and the tangential traction σ_t on the interface, are

$$\begin{aligned}&(\sigma_n)_l - (\sigma_n)_a = (\sigma_{ij}n_j n_i)_l - (\sigma_{ij}n_j n_i)_a \\ &= -(p_l - p_a) + 2\mu_l\mathbf{n}\cdot(\frac{\partial\mathbf{u}}{\partial n})_l - 2\mu_a\mathbf{n}\cdot(\frac{\partial\mathbf{u}}{\partial n})_a \\ &= \Gamma\kappa,\end{aligned} \tag{4}$$

$$\begin{aligned}&(\sigma_t)_l - (\sigma_t)_a = [(\sigma_{ij}n_j)_l - (\sigma_{ij}n_j)_a]t_i \\ &= \mu_l\left(\mathbf{t}\cdot\frac{\partial\mathbf{u}}{\partial n} + \mathbf{n}\cdot\frac{\partial\mathbf{u}}{\partial t}\right)_l - \mu_a\left(\mathbf{t}\cdot\frac{\partial\mathbf{u}}{\partial n} + \mathbf{n}\cdot\frac{\partial\mathbf{u}}{\partial t}\right)_a \\ &= 0,\end{aligned} \tag{5}$$

where σ_{ij} (i and j=1, 2, 3) are the stresses in the fluid (subscript l denotes the liquid, subscript a denotes the air), n_i (i=1, 2, 3) are components of $\mathbf{n}$, and $\mathbf{t}$ is a unit vector tangent to the liquid-air interface.

The *continuous-surface-force* (CSF) model of Brackbill, Kothe, and Zemach (1992) is used to mimic the surface effect of the liquid-air interface. The model treats surface tension as a continuous 3-dimensional force rather than a boundary condition across the interface. The free surface is tracked by the advection scheme for volume fraction. Thus the boundary-value problem at the interface is replaced by an approximate continuous model as follows: The fluid density ρ, which takes the value of ρ_l in the computational cells containing only liquid and the value ρ_a in the cells containing only air, changes discontinuously at the interface. In the CSF model by Brackbill, Kothe, and Zemach (1992), the discontinuous function ρ is replaced by a smooth variation of ρ from ρ_a to ρ_l over a distance of length comparable to the computational mesh space Δx. The values of ρ are specified at rid points and interpolated between. One then approximates the pressure jump induced by surface tension at the interface by an equivalent volume force $\mathbf{F}_{sv}$ over the transition region. This is accomplished by replacing the momentum equation Eq. (1) in the transition region by

$$\rho\frac{d\mathbf{u}}{dt} = -\nabla p + \mathbf{F}_{sv} + \rho\mathbf{g} + \mu\nabla^2\mathbf{u}, \tag{6}$$

$$\mathbf{F}_{sv} = \Gamma\kappa\nabla\rho, \tag{7}$$

where μ is the mixture viscosity, and the surface curvature κ is defined in Eq. (3) with the surface normal being

$$\mathbf{n} = \frac{\nabla\rho}{|\nabla\rho|}. \tag{8}$$

Note that the volume force is localized that it is zero outside the interface transition region where ρ is constant.

The effects of wall adhesion at fluid interfaces in contact with rigid boundaries in equilibrium can be estimated within the framework of the CSF model in terms of θ, the equilibrium contact angle between the fluid and wall. The normal to the interface at points $\mathbf{x}_w$ on the wall is

$$\mathbf{n}_{wall}\cos\theta + \mathbf{n}_t\sin\theta = \mathbf{n}, \tag{9}$$

where $\mathbf{n}_t$ lies in the wall and is normal to the contact line between the interface and the wall at $\mathbf{x}_w$, and $\mathbf{n}_{wall}$ is the unit wall normal directed into the wall. The unit normal $\mathbf{n}_t$ is computed using Eq. (8) at the wall.

The advection of the volume fraction of the liquid F is based on the discrete conservation equations [Zwart (2003)] for the phasic continuity:

$$\frac{\partial F}{\partial t} + \nabla\cdot\mathbf{u}F = 0. \tag{10}$$

The function F specifies the fracture of the volume in each computational cell occupied by the fluid. The proportions of liquid and air in the mixture determine the average density and viscosity in a computational cell.

3 Computational Model

The general fluid analysis software CFX (ANSYS, Canonsburg, PA) was used for the numerical simulation. The computational model is shown in Fig. 1. A cylindrical capillary tube of rectangular cross-section with a rectangular entrance, and with an exit opening a at the top end or on the side wall is shown in Fig. 1(B). The exit opening is also a rectangle. The mesh of the model was generated by ANSYS (ANSYS, Canonsburg, PA). Blood enters the capillary tube from the bottom, and flows to the exit opening a as illustrated in Fig. 1(B). The computational model involves two fluids: the blood and the air. The capillary tube is rigid and is dipped 1 mm into a drop of blood as shown in Fig. 1(C). The volume of a drop of blood is 120 times larger than that of the capillary

tube. The blood volume used in the numerical model is 540 mm^3 (with length 4 mm, thickness 9 mm, and width 15 mm), while the same volume of air is used outside the capillary exit. The capillary tube is stationary in the perpendicular position. Constant atmospheric pressure (1 atmospheric pressure) is assumed around the air volume surrounding the exit opening and on the blood free-surface outside the tube. Hydrostatic pressure is used on the blood boundaries far from the tube. The tube entry is deep in the blood for 1 mm, there is no boundary condition applied on the tube entry and at the exit opening. The initial conditions are that the liquid-air interface is flat and that the fluids are stationary. Taking advantage of symmetry, a quarter of the model as shown in Fig. 1(C) is used in the computation for the capillary tube with a top exit, and a half of model for the capillary tube with a side exit opening. The mesh of the quarter model has a total of 31827 nodes and 27944 cells.

For the convenience of comparisons among simulation results, three dimensionless quantities are introduced:

$$\text{Normalized exit opening area } A' = \frac{a}{A_c}, \tag{11}$$

Normalized average liquid surface height

$$H' = \frac{H}{h/2}, \tag{12}$$

Normalized locations of the exit opening on the side wall

$$C' = \frac{c}{L}, \tag{13}$$

where a is the area of an exit opening, A_c is the cross sectional area of the capillary tube and is equal to $b \times h$, H is the average height of the liquid surface in the capillary tube, h and L are the thickness and length of the capillary tube, respectively, and c is the distance from the center of the exit opening on the side wall to the top of the tube. The following dimensions of the tube were used: width b=1.5 mm, thickness h=0.5 mm, and length L=6 mm mm. The exit area a, and its location c were varied in the simulations to examine their effects on the flow of blood in the capillary tube.

As shown in Eq. (3), the magnitude of the surface tension force is dependent on the surface tension coefficient Γ and the surface curvature κ. The surface curvature is the gradient of the surface normal vector and is related to the wetting angel. In the computation, Γ is taken as 0.04 N/m. We also assume the contact angle to be 0.01°. When the gravity is considered, the gravitational acceleration 9.81 m/s^2 was adopted. The basic material constants used for blood are: the mass density of blood $\rho = 10^3$ kg/m^3, the dynamic viscosity coefficients of blood $\mu_l = 0.004$ kg/(m·s)., and the dynamic viscosity coefficient of air $\mu_a = 1.725 \times 10^{-5}$ kg/(m·s).

In our analysis, the surface tension and the gravitation force are the only driving forces. The flow occurs at room temperature under normal atmosphere pressure. Hence, at the exit and on the free surface of the body of the fluid, the reference pressure is the standard atmosphere pressure of 10^5 Pa. The heat transfer effect is ignored. The no-slip condition is applied at the tube walls except the liquid/air interface. On the planes of symmetry, the normal velocity is zero.

4 RESULTS

4.1 Effects of the area and location of capillary tube exit openings on the blood flow movement as functions of time.

The blood is pull upward by surface tension after the capillary tube is dipped into the blood. The results shown in Fig. 2 are cases for a square exit opening, and viscosity μ=4 cp, with the gravity neglected.

Fig. 2 demonstrates that the area and location of the exit openings affect the movement of blood flow in the capillary tubes. A' is the ratio between the area of an exit opening a and the cross-sectional area of the capillary tube. The result of A'=1 is from our previous article [Huang, Bhullar, and Fung (2001)]. The moving of blood flow in the capillary tubes is slower when A'=0.0395 than that when A'=1. With same exit opening areas, blood flow in the tube with an exit opening at the top end is faster than that at the side wall. When the exit opening at the side wall is far away from the top end of the tube, the moving of blood flow in the tube is much slower. Here, we tested three cases, in which $C' = 0.0368$, 0.13481, and 0.23285. C' is the ratio between the distance from the center of the exit opening on the side wall to the top of the tube$c$ and the length of the capillary tube L. A bigger C' value indicates a bigger distance from the center of the exit opening to the top end of the tube. In these three cases, the slowest moving of blood flow happens when C'=0.2329.

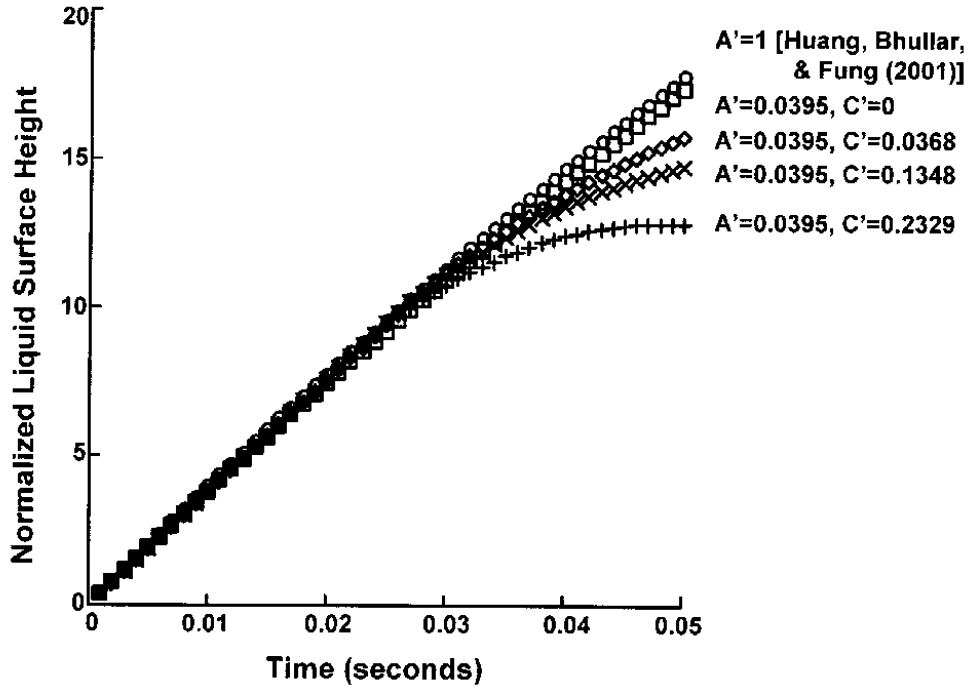

Figure 2 : Effects of the areas and locations of capillary tube exit openings on the blood flow movement (normalized liquid surface height) as functions of time. See text for more details.

4.2 Movement of blood flow in the capillary tube as functions of the exit opening area.

In Fig. 3, the normalized liquid surface height is plotted against the normalized exit opening area A' at t=0.05 s for the cases with an exit opening at the top end of the tube (C'=0) and an exit opening at the side wall of the tube (C'=0.0368). The data were fit with a formula: $a_1 + a_2\,[1-\exp(-a_3 x)]$, where a_1, a_2, a_3 are constants.

Flow of blood in the capillary tube with an exit opening at the top end is faster than that at the side wall. The moving of blood flow in the capillary tube is much slower in the tubes with the exit opening area less than 5% of the cross-sectional area of the tube, but will not have significant difference if the exit opening area is larger than 10% of the cross-sectional area of the tube. Our results demonstrate that the exit opening areas affect the movement of blood flow in the capillary tubes when the exit opening area is less than 10% of the cross-sectional area of the tube.

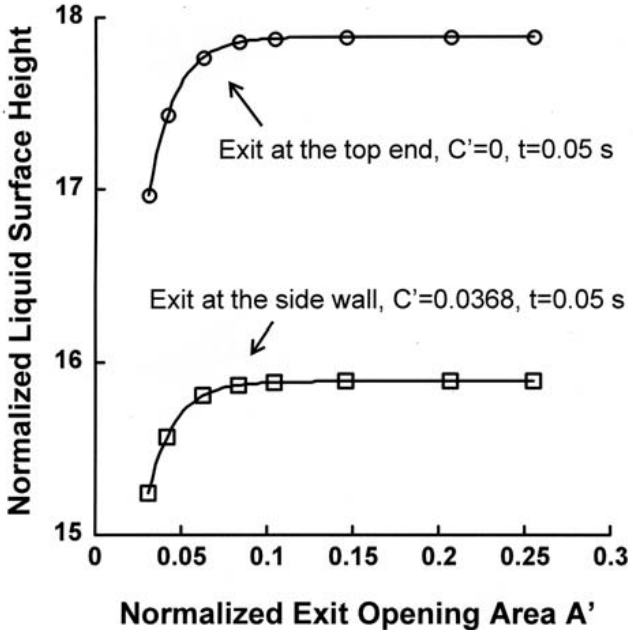

Figure 3 : Effects of the exit opening areas and locations on the blood flow movement (normalized liquid surface height) as functions of the normalized exit opening area A'. See text for more details.

4.3 Comparison between the analytical model in Huang, Bhullar, and Fung (2001) and the finite element model of the present paper.

The surface-tension-driven flow of blood in a long tube of rectangular cross section was analyzed in both our analytical model in Huang, Bhullar, and Fung (2001) and 3-dimentional finite element model in the present article. The difference between these two solutions is due to three reasons: (1). The capillary tube in the present paper has a closed end with a small open window, but has an open end in Huang, Bhullar, and Fung (2001). (2). The initial stage of the development of the interface when the tube first touched the blood drop was analyzed in detail in Huang, Bhullar, and Fung (2001), but was sidestepped in the present paper. (3). The dynamic resistance to the flow of the air in front of the blood-air interface is analyzed in detail in the present paper, but was ignored in Huang, Bhullar, and Fung (2001) because of the smallness of the density and coefficient of viscosity of air in comparison with those of the blood. The numerical differences of the final results are shown in Fig. 2. It is seen that in the case of end window, the differences of the interface movement are less than 5%. The air slows down the interfacial movement by a few percent ($<$5%). The case of side window cannot be solved by the method of Huang, Bhullar, and Fung (2001). The finite element model is the method of choice to deal with the complex boundary conditions.

5 Discussion

Many parameters can affect the flow of blood in the capillary tube. Some examples have been examined in Huang, Bhullar, and Fung (2001). In this paper, we examined the effects of the exit port (i.e., area and location of exit opening) on the flow of blood in the capillary tube with numerical simulation. Blood is assumed to be a Newtonian fluid. Blood rheology is significantly non-Newtonian under two circumstances [Fung (1993)]: (1) When the characteristic dimension of the flow channel is equal to or smaller than the diameter of the red blood cell. (2) When the shear strain rate is smaller than a certain value. We propose the following design principles for any instrument for glucose measurement: (1) The diameter of the tube must be larger than the erythrocyte diameter. (2) The port of exit must be sufficiently large so that the shear strain rate is large enough for the blood rheology to be Newtonian. The results of our previous [Huang, Bhullar, and Fung, (2001)] and present studies will enable the instrument designer to select the tube diameter and the exit port size as function of the surface tension. Hence they are helpful tools for the design of blood glucose measuring instruments. A design that works in the non-Newtonian regime would be interesting also, but then the analysis of flow will be more complicated. The contact angle θ between the solid wall and the blood-air interface is another important parameter. Unfortunately the values for different liquids and solids are not well known, and not listed in authoritative handbooks. Filling this gap of knowledge would be important.

6 Conclusion

The finite element computation can yield detailed information. If the capillary tube has an open window at the end, the simplified analytical solution of Huang, Bhullar, and Fung (2001) yields results within 5% of the numerical solution by finite elements. If the capillary tube has a closed end and a window on the side wall, the effect of the air motion in front of the blood-air interface is more significant.

Acknowledgement: W. Huang would like to acknowledge the support from the National Heart, Lung and Blood Institute of the National Institutes of Health, the NASA Goddard Space Flight Center, and the National Health Research Institutes (Taiwan). R. S. Bhullar wishes to thank Dr. Jorg Schreiber and Mr. Douglas P. Walling of Roche Diagnostics Corporation for their encouragement and foresight.

References

Brackbill, J. U.; Kothe, D. B.; Zemach, C. (1992): A continuum method for modeling surface tension. *J. Comput. Phys.*, vol. 100, pp. 335-354.

Fung, Y. C. (1975): Does the surface tension make the lung inherently unstable? *Circ. Res.* vol. 37, pp. 497-502.

Fung, Y. C. (1990): How does the baby catch its first breaths? In: G. T. Yates (ed) *Engineering Science: Fluid Dynamics*, World Scientific Publishing Co., Singapore, pp. 135-145.

Fung, Y. C. (1993): *Biomechanics: Mechanical Properties of Living Tissues*, Springer, New York, pp. 66-105.

Fung, Y. C. (1997): *Biomechanics: circulation*, Springer, New York. pp. 291-307.

Huang, W.; Bhullar, R. S.; Fung, Y. C. (2001): The surface-tension-driven flow of blood from a droplet into a capillary tube. *J. Biomech. Eng.*, vol. 123, pp. 446-454.

Lew, H. S.; Fung, Y. C. (1969): On the low-Reynolds-number entry flow into a circular cylindrical tube. *J. Biomech*, vol. 2, pp. 105-119.

Purday, H. F. P. (1949): *An introduction to the mechanics of viscous flow (Sreamline flow)*, Dover Publications Inc., New York.

Thurston, G. B. (1976): The viscosity and viscoelasticity of blood in small diameter tubes. *Microvas. Res.*, vol. 11, pp. 133-146.

Tong, P.; Fung, Y. C. (1965): The effect of wall elasticity and surface tension on the forced osillations of a liquid in a cylindrical container. In: H. Cohan, and M. Rogers (eds) *Fluid Mechanics and Heat Transfer Under Low Gravity*, Lockheed Corp., Los Angeles, pp. 11-41.

Yih, C. S. (1988): *Fluid Mechanics: A Concise Introduction to the Theory*, West River Press, Ann Arbor, MI.

Zupkas, P. (1977): Mathematical analysis of surface tension diagrams of mammalican lung components, M.S. thesis, University of California, San Diego.

Zwart, P. J. (2003): Free surface flow modelling of an impinging jet. In: ASTAR International Workshop on Advanced Numerical Methods for Multidimensional Simulation of Two-Phase Flow. Sep. 15-16, GRS Garching, Germany.